

RESEARCH

Open Access



Scutellaria barbata D.Don and *Hedyotis diffusa* Willd herb pair combined with cisplatin synergistically inhibits ovarian cancer progression through modulating oxidative stress via NRF2-FTH1 autophagic degradation pathway

Xue Sui^{1†}, Bingqing Gao^{1,2†}, Liu Zhang^{1,3}, Yanmin Wang¹, Junnan Ma¹, Xingchen Wu¹, Chenyu Zhou¹, Min Liu^{4*} and Lin Zhang^{1*}

Abstract

Background Cisplatin (DDP) is one of the most effective anticancer drugs, commonly used to treat advanced ovarian cancer (OC). However, DDP has significant limitations of platinum-based drugs, including chemical resistance and high-dose toxic side effects. Traditional Chinese medicines (TCMs) often presented in the form of formula, in which the herb pair was the basic unit. *Scutellaria barbata* D.Don and *Hedyotis diffusa* Willd (SB-HD) are famous TCMs herb pair that have been shown to help treat multiple types of cancers. However, the synergistic effects and mechanism of combination of SB-HD and DDP to enhance DDP chemosensitivity in OC are still unknown.

Results In vitro, we found that the optimal proportion of SB-HD to inhibit the proliferation of OC cells was 2:1, SB-HD and DDP were shown to synergistically reduce the viability of OC cells, inhibit the colony formation, promote cell cycle arrest and apoptosis, as well as inhibit cell migration and invasion. In vivo, combination treatment significantly inhibited the growth of subcutaneous tumors in BALB/c nude mice and reduced the toxic side effects of DDP. Mechanistically, SB-HD and DDP combination treatment significantly promoted oxidative stress response, decreased MMP, inhibited ATP production, decreased ROS levels and increased SOD activity, increased the expression of NRF2, HO-1, ATG5 and LC3, decreased the expression of p62 and FTH1 both in OC cells and tumor tissue of mice. Inhibitor 3-MA (Methyladenine, autophagy inhibitor) and Fer-1 (Ferrostatin-1, iron ion inhibitor) can effectively

[†]Xue Sui and Bingqing Gao contributed equally to this work.

*Correspondence:

Min Liu
15040578452@163.com
Lin Zhang
zhl8247@163.com

Full list of author information is available at the end of the article



© The Author(s) 2024. **Open Access** This article is licensed under a Creative Commons Attribution-NonCommercial-NoDerivatives 4.0 International License, which permits any non-commercial use, sharing, distribution and reproduction in any medium or format, as long as you give appropriate credit to the original author(s) and the source, provide a link to the Creative Commons licence, and indicate if you modified the licensed material. You do not have permission under this licence to share adapted material derived from this article or parts of it. The images or other third party material in this article are included in the article's Creative Commons licence, unless indicated otherwise in a credit line to the material. If material is not included in the article's Creative Commons licence and your intended use is not permitted by statutory regulation or exceeds the permitted use, you will need to obtain permission directly from the copyright holder. To view a copy of this licence, visit <http://creativecommons.org/licenses/by-nc-nd/4.0/>.

reverse the expression changes of the key target proteins, but not ZnPP (Zinc protoporphyrin, HO-1 inhibitor). Through bioinformatics analysis, it was found that the abnormal expression level of NRF2 and FTH1 mRNA has a high prognostic value, at the same time, the other four key proteins respectively or interacting with NRF2 and FTH1, also play important roles in the occurrence and development of OC.

Conclusion Our findings uncover a synergistic effect of SB-HD and DDP against OC through modulating oxidative stress via NRF2-FTH1 autophagic degradation pathway, which may provide an important theoretical foundation for the use of SB-HD and a new strategy for enhancing DDP chemosensitivity as well as reducing toxic side effects.

Keywords *Scutellaria barbata* D.Don and *Hedyotis diffusa* Willd, Ovarian cancer, DDP chemosensitivity, NRF2/HO-1, Oxidative stress, Ferritin autophagic degradation

Introduction

As the global incidence of cancer continues to rise, cancer has become one of the leading causes of death in all countries of the world, and also indicates that it has become an important obstacle to improving human life expectancy [1]. Worldwide, OC is the seventh most common cancer, and because of the lack of reliable symptoms and biomarkers in the early stage, most OC patients die of advanced disease with peritoneal metastasis and poor prognosis, making it the eighth most common cause of cancer death in women and the second most common cause of gynecological cancer death (Second only to uterine cancer) [2]. Platinum-based drugs, such as DDP, are among the most effective anticancer drugs and are commonly used to treat advanced OC [3, 4]. However, significant limitations of platinum-based drugs include the acquisition of resistance in initially responsive tumors and the development of serious side effects at higher doses [3, 4]. Therefore, the research of drugs that can inhibit the activity of OC is still the focus of all walks of life, and there is still an urgent need to study safe and effective alternative anti-cancer methods in clinic, such as the combination of food and herbal supplements with current chemotherapy, in order to improve the therapeutic effect of existing drugs.

Plant medicine is rich in resources, as a natural medicine. In the theory of traditional Chinese medicine (TCM), Toxic Heat, which is similar to tumorigenic factors, is one of the main causes of tumors. Modern studies have shown that heat-clearing and detoxifying herb drugs have the effects of clearing heat, detoxifying, antibacterial and anti-inflammatory, improving immunity and anti-tumor, so they have become an important part of TCMs prescriptions for the treatment of tumors [5]. Among them, SB and HD are famous TCMs herb pair of heat-clearing and detoxifying herb drugs that have been shown to help treat multiple types of cancers. And, it has been reported that the extracts of SB and HD can inhibit the growth of OC cells and promote the apoptosis of OC cells in a dose-dependent manner, respectively, but have no significant effect on normal ovarian cells [6, 7].

Autophagy is an intracellular metabolic process, which maintains the stability and balance of the intracellular environment by decomposing and recycling the aging or abnormal organelles in cells [8]. Oxidative stress is a state of imbalance between oxidative and antioxidant reactions in vivo, accompanied by the production of a large number of oxidative intermediates [9]. Oxidative stress leads to autophagy, which plays an important role in the development of cancer and is one of the important ways for cells to survive and adapt to the environment [9, 10]. Nuclear factor erythroid 2 related factor 2 (nuclear factor erythroid 2, Nrf2) is an important molecule that regulates the expression of anti-inflammatory, anti-apoptotic and anti-oxidant genes in cells, and regulates the transcription of downstream factors such as heme oxygenase 1 (HO-1) [11–13]. HO-1, as an inducible enzyme, is considered a measurable indicator of oxidative stress, which oxidizes cellular heme to carbon monoxide (CO), biliverdin/bilirubin, and ferrous iron [9]. The heme oxygenase reaction may exhibit cytoprotective effects through its metabolites biliverdin/bilirubin and CO against oxidative attacks, by scavenging or neutralizing ROS, anti-inflammatory and so on, while ferrous iron possesses pro-oxidant activity [9].

Ferroptosis is a form of cell death characterized by iron-dependent and lipid peroxidation [14]. Ferritinophagy is the upstream regulatory mechanism of ferroptosis, and the excessive activation of ferritinophagy will promote the occurrence of ferroptosis [14]. When the expression of FTH1 subunit of ferritin decreases, the amount of iron storage decreases, and the increase of free iron content will lead to cell death [14]. It was found that the autophagy degradation of FTH1 mediated by AKT1 deletion would lead to the sensitivity of cisplatin-resistant OC cells to ferroptosis [15]. In pancreatic cancer, activation of the Atg5/Atg7-NCOA4 axis will inhibit FTH1 expression and promotes ferritinophagy, triggering a cascade to induce pancreatic adenocarcinoma cell death [16]. Other studies have found that Itaconic acid can reduce the expression of FTH1 in pancreatic cancer, and with the increase of LC3 level, it can activate ferritin autophagic degradation to play an anti-tumor role [17].

At present, by annotating the metabolic pathways of proteome and transcriptome in the early stage, and analyzing the correlation and integration of the annotated proteins and genes in the same pathway, our research team has obtained two series of KEGG pathways which are significantly enriched in two omics, respectively. Among them, it is suggested that ferroptosis may play an important role in the death of OC cells induced by SB-HD. In addition, preliminary experiments have been carried out, it was confirmed that ferritinophagy is an important mechanism in this process. However, the synergistic effects and mechanisms of combination of SB-HD and DDP to enhance DDP chemosensitivity in OC are still unknown. Herein, the *in vitro* and *in vivo* inhibitory action of SB-HD in combination with DDP on OC cells were assessed in this study.

Materials and methods

Materials

DDP was purchased from Shanghai Aladdin Biochemical Technology Co., Ltd. (Shanghai, China). The SB and HD were purchased from Beijing Tongrentang Pharmacy Co., LTD (Beijing, China). OC cell lines SKOV3 and OVCAR3 were obtained from Wuhan Pricella Biotechnology Co., Ltd. (Wuhan, China). CCK-8 and Hoechst Staining Kit were purchased from Jiangsu KeyGEN BioTECH Corp., Ltd (Nanjing, China). Cell cycle Assay Kit, cell apoptosis Assay Kit, mitochondrial membrane potential (MMP) Assay Kit, ROS Assay Kit, ATP Assay Kit, and SOD Assay Kit were purchased from Beyotime Biotechnology (Shanghai, China). Antibodies of NRF2, HO-1, and ATG5 were purchased from Shenyang Wanlei Life Sciences Co., Ltd. (Shenyang, China). Antibodies of FTH1 and LC3 were purchased from Cell Signaling Technology (USA). And p62 antibody was purchased from Wuhan Servicebio Technology Co., Ltd. (Wuhan, China). Antibodies of Ki67 and β -actin were purchased from ABclonal Biotech Co., Ltd (Wuhan, China). Fer-1 was obtained from Selleck Chemicals (USA). ZnPP and 3-MA were obtained from MedChemExpress (USA). ALT Assay Kit, AST Assay Kit, BUN Assay Kit, and CRE Assay Kit were purchased from Nanjing Jiancheng Bioengineering Institute (Nanjing, China).

Animals

6–8-week-old female BALB/c nude mice (18–22 g) were used in all experiments. All animals were group-housed under controlled temperature ($22\text{ }^{\circ}\text{C} \pm 1\text{ }^{\circ}\text{C}$) and relative humidity ($50\% \pm 5\%$) on a 12 h:12 h light/dark cycle, with free access to water and chow. All animal experiments were performed conforming to the NIH Guide for the Care and Use of Laboratory Animals and in accordance with the guidelines approved by the Institute for Animal Care and Use Committee in Dalian Medical University.

Preparation of SB-HD extract freeze-dried powder

The SB and HD used in this study had been identified by experienced Chinese medicine experts. The usage of each crude herb was accurately weighed as follows: Prepared SB and HD in a 2:1 mass ratio. They were mixed and a total of mixture was extracted 2 times in a reflux extraction device, with a volume of water equal to ten times the weight of the herb at the first round, reduce by half in the second round. After the extracting solutions were mixed and filtered with four-layer absorbent gauze, the final volume of the solution is recorded. Then the mixture was frozen inside a $-80\text{ }^{\circ}\text{C}$ refrigerator and freeze dried in a freeze drier to give a fine powder. Accurately weighed extraction powder (1 g) was transferred into a 100 ml serum-free culture medium and was filtered through $0.22\text{ }\mu\text{m}$ filter in subsequent experiments. The preparation of other proportions (4:1, 1:1, 1:2, 1:4) of SB-HD is the same as above.

Cell viability assay

SKOV3 and OVCAR3 cells were seeded into 96-well plates (8,000 cells/well) and incubated for 24 h. After the cells were treated with drugs, the medium was replaced with $100\text{ }\mu\text{l}$ fresh medium containing $10\text{ }\mu\text{l}$ CCK-8 reagent. After incubation for 2 h, the absorbance was measured at 450 nm using Microplate reader.

Colony formation assay

SKOV3 and OVCAR3 cells were seeded into 6-well plates (800 cells/well) and incubated for 24 h. After the cells were treated with drugs for 24 h, the medium was replaced with fresh medium containing 10% FBS for 10–14 days, change the medium every 2 or 3 days during this period. The colonies were fixed in methanol for 20 min and were stained with 1% crystal violet for 20 min, then were slowly washed with running water, air dried at room temperature and photographed.

Hoechst staining assay

SKOV3 and OVCAR3 cells were seeded into 6-well plates (1×10^5 cells/well) and incubated for 24 h. After the cells were treated with drugs for 24 h, the cells were fixed for 15 min by 4% paraformaldehyde after washing 3 times using ice-cold PBS, and then stained with Hoechst 33,342 for 10 min. Being washed twice with PBS, the cells were immediately photographed under a fluorescence microscope at $\times 400$ magnification.

Detection of cell cycle, cell apoptosis and MMP

SKOV3 and OVCAR3 cells were seeded into 6-well plates (3×10^5 cells/well) and incubated for 24 h. After the cells were treated with drugs, cell cycle, cell apoptosis and MMP were measured according to the manufacturer's

instructions for each kit. The data were obtained using an FACSVerse Flow Cytometer.

ROS levels, ATP content and SOD activity measurement

SKOV3 and OVCAR3 cells were seeded into 6-well plates (3×10^5 cells/well) and incubated for 24 h. After the cells were treated with drugs, ROS levels, ATP content and SOD activity were measured according to the manufacturer's instructions for each kit. The data of ATP and SOD were obtained using Microplate reader, the ROS assay data were obtained using an FACSVerse Flow Cytometer.

Wound healing assay

SKOV3 and OVCAR3 cells were seeded into 6-well plates (3×10^5 cells/well). Until cells 80% confluence, a scratch across the center of the monolayer was made using a 200 μ l pipette tip. After gently washing the wells twice, the cells were cultured in a medium with drugs. The area of scratch was photographed at 0 h and 24 h.

Transwell migration and invasion assays

For transwell migration assays, SKOV3 and OVCAR3 cells were seeded into Transwell insert (2×10^4 cells/well) and cultured in serum-free medium for 6 h. For transwell invasion assays, the insert membrane was coated with Matrigel[®] Matrix and incubated in the incubator at 37°C for 1–4 h, then the cells were seeded. Subsequently, the cells in the upper chamber were treated with drugs, and the upper chambers were put into the (lower) wells containing fresh medium containing 20% FBS. After the cells were treated with or without drugs for 18 h, the upper side of the insert membrane was cleansed with a cotton swab to remove the cells that had not passed through the membrane. The cells on the lower surface of the insert membrane were fixed in methanol for 20 min and stained with 1% crystal violet for 20 min. The number of migration and invasion cells was manually counted under the inverted microscope and statistically analyzed with the ImageJ software.

Xenotransplantation experiment

SKOV3 cells (1×10^7) suspended with Matrigel[®] (Xiamen Mogeng; 100 μ l total volume) in a 1:1 mixture was injected subcutaneously into nude mice for xenograft formation. Two weeks later, the animals were randomly divided into four groups with six mice in each group and were then treated as follows: (1) Control group, gavage of an equal volume of water and injection of an equal volume of normal saline; (2) DDP group, intraperitoneal administration was performed every 3 days (3 mg/kg); (3) SB-HD group, gavage administration was performed every day (16 g/kg); (4) DDP+DB-HD group, both intraperitoneal and gavage administration as DDP group and

DB-HD group. Mice weight and tumor volumes were measured every 3 days. Tumor volume was calculated as $1/2 \times \text{length} \times \text{width}^2$. After 16 days, all mice were sacrificed. Blood was collected for biomedical measurement. Tumors and organs were collected and weighed.

Biomedical measurement

Serum levels of alanine aminotransferase (ALT), aspartate amino-transferase (AST), blood urea nitrogen (BUN), and creatinine (Cre) were measured according to the manufacturer's instructions for each kit.

Histology and immunohistochemistry (IHC)

The dissected tumors and organs were paraffin embedded and cut into sections for HE staining. For immunohistochemistry (IHC) staining, the tumor sections were deparaffinized, hydrated, antigen retrieved, and then incubated with the primary antibody followed by the incubation with the secondary antibodies for 1 h in the next day. Finally, observed under a microscope and photographed.

Western blotting analysis

Western blotting was performed as previously described. In simple terms, the cultured cells and tumor tissues and were lysed with ice-cold RIPA Lysis Buffer containing protease inhibitors Cocktail and PMSF for 30 min. The concentrations of protein were determined by a Pierce BCA protein assay kit. Equal amounts of proteins were separated with 8–15% SDS-PAGE, and then transferred to a PVDF membrane for blotting. The membranes were washed and blocked with 5% BSA, and then incubated with primary antibody solution overnight at 4°C. Finally, the membranes were incubated with the corresponding secondary antibodies conjugated to HRP for 1 h at room temperature and visualized by multifunctional gel imaging analysis system.

Bioinformatics analysis

The transcriptional expression patterns, clinical stages, survival rate, prognostic values, genetic alterations and genetic interrelations of six key genes in OC patients were investigated using a range of databases: Gene Expression Profiling Interactive Analysis (GEPIA) (<http://gepia.cancer-pku.cn/>), and Kaplan-Meier Plotter (<http://kmplot.com/analysis/>). Finally, the results are visualized.

Statistical analysis

All data are reported as the mean \pm standard error of the mean (SEM). Data statistical analysis is performed using GraphPad Prism software. The two-tailed Unpaired Student's t-test, one-way ANOVA, or two-way ANOVA with Tukey or Bonferroni *post hoc* test were used as indicated $p < 0.05$ were considered statistically significant.

Results

SB-HD enhanced the cytotoxicity of DDP for OC cells and inhibited colony formation

Modern pharmacological studies have confirmed that the pairing ratio of the active site for herbal medicines usually affects efficacy. Therefore, we prepared five SB-HD freeze-dried powders at different mass ratios (1:1, 1:2, 2:1, 1:4, 4:1), and were investigated in the following two cell lines: SKOV3 and OVCAR3. The average IC₅₀ values of compatibility ratio 4:1, 2:1, 1:1, 1:2, and 1:4 for SKOV3 cells were 2.904, 3.176, 3.505, 3.714 and 3.561 mg/ml, respectively, the order of the inhibition strength is: 4:1 > 2:1 > 1:1 > 1:4 > 1:2 (Fig. 1A-B). The average IC₅₀ values of compatibility ratio 4:1, 2:1, 1:1, 1:2, and 1:4 for OVCAR3 cells were 4.171, 3.849, 5.313, 4.894 and 4.280 mg/ml, respectively, the order of the inhibition strength is: 2:1 > 4:1 > 1:4 > 1:2 > 1:1 (Fig. 1A-B). Based on the above results, according to the important principle that

the therapeutic dose of drugs is generally between the minimum effective dose and the maximum dose, and the smaller effective dose is used in the initial treatment, we choose the SB-HD ratio of 2:1 as the compatibility ratio of herb pair in the next experiments, at concentrations of 3, 4 and 5 mg/ml. As shown in Fig. 1C, we detected the cell viability of OC cells treated with SB-HD (2:1) at 6 h, 12 h, 24 h, 48 h and 72 h, respectively, and the 24 h were subjected to subsequent studies.

Next, we evaluated the anti-tumor effect of SB-HD and DDP combination for OC cells by CCK-8 assay. As shown in Fig. 1D-E, SB-HD synergistically promoted the inhibitory effect of DDP on OC cells, with various concentrations of DDP. The average IC₅₀ values for SKOV3 and OVCAR3 cells treated with DDP alone were 14.19 and 8.579 μg/ml. The average IC₅₀ values for SKOV3 and OVCAR3 cells treated with SB-HD and DDP combination were 8.980 and 5.860 μg/ml. Based on the above

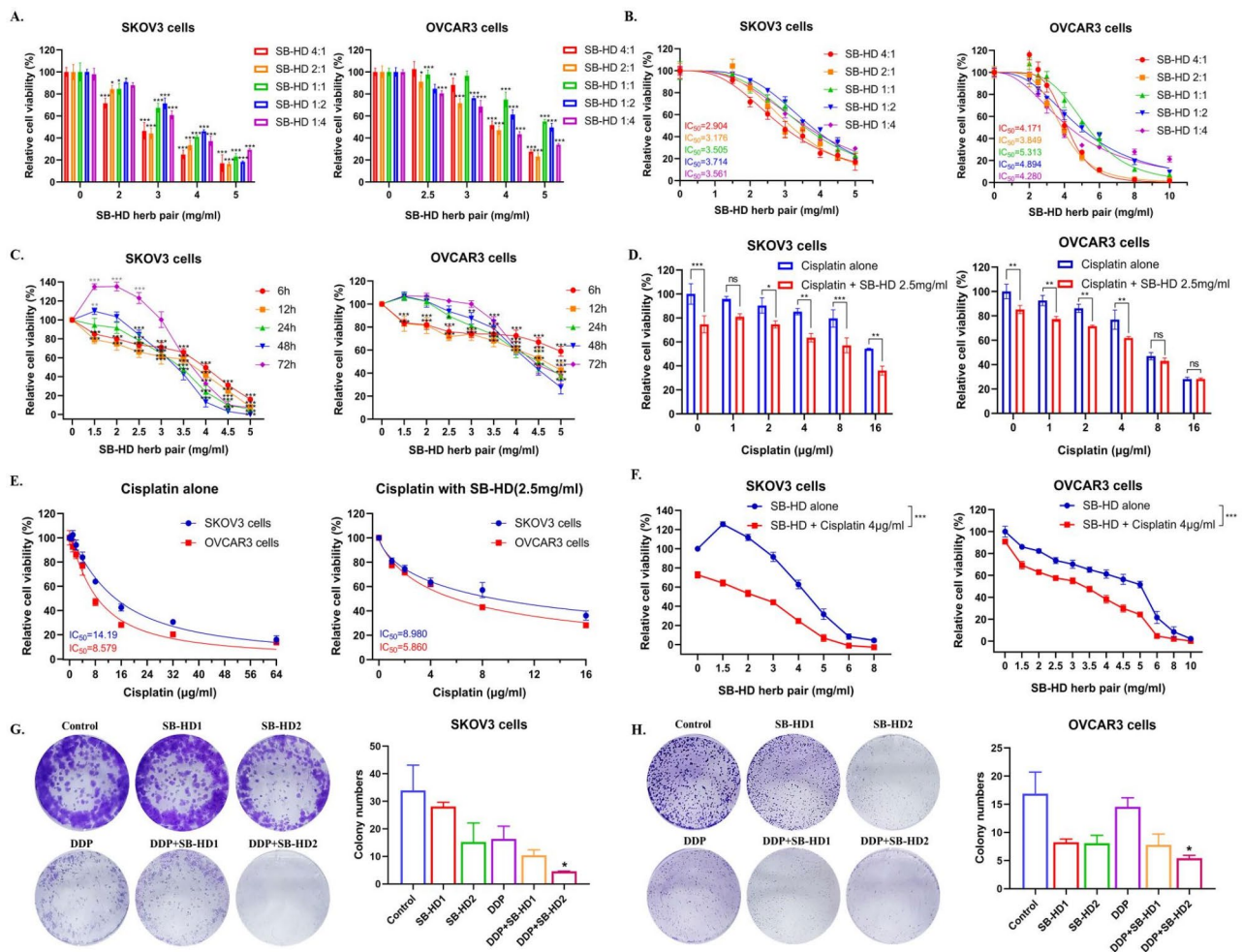


Fig. 1 SB-HD enhanced the cytotoxicity of DDP for OC cells and inhibited colony formation. (A–B) Cell viability of SKOV3 and OVCAR3 cells after treatment with indicated concentrations of SB-HD at different mass ratios (4:1, 2:1, 1:1, 1:2, 1:4). (C) Time-dependent curves of cell viability by SB-HD at 6 h, 12 h, 24 h, 48 h, and 72 h. (D–F) Cell viability of SKOV3 and OVCAR3 cells after combination treatment of SB-HD and DDP. (G–H) Clone formation of SKOV3 and OVCAR3 cells treated with SB-HD and DDP (* $p < 0.05$, ** $p < 0.01$, *** $p < 0.001$ vs control; # $p < 0.05$, ## $p < 0.01$, ### $p < 0.001$ vs DDP; $n = 3-6$)

results and reviewing the relevant literature, the concentration of DDP 4 $\mu\text{g/ml}$ is used as the concentration for combination treatment on OC cells in subsequent studies. Meanwhile, DDP also synergistically promoted the inhibitory effect of SB-HD on OC cells, with various concentrations of SB-HD (Fig. 1F). These indicate that SB-HD and DDP have a combined inhibitory effect on OC.

Further, it observed that the individual drugs alone and combination all inhibited colony formation, the combination of the two drugs at high concentrations of SB-HD induced a significant decrease in colony formation comparing with the control treatment (Fig. 1G-H).

SB-HD alone and in combination with DDP promoted cell cycle arrest and apoptosis

As we have confirmed, SB-HD enhanced the cytotoxicity of DDP for OC cells and inhibited cell proliferation. In addition, the cell cycle regulates cell proliferation, so we examined the effects of SB-HD alone and in combination with DDP on cell cycle progression. As shown in Fig. 2A-D, SB-HD alone and in combination with DDP blocked the cell cycle in S phase. These results further suggest that combination treatment inhibited OC cells proliferation. Subsequently, we assessed the antitumor activities via induction of apoptosis by Hoechst staining assay, as shown in Fig. 2E, cells displayed a uniformly blue fluorescence in every group, and combination treated cells showed more bright blue dots in the nuclei than other groups. So, we next determined apoptotic event by performing Annexin V and PI fluorescent staining and detecting with flow cytometer. The results showed that apoptosis clearly occurred after the treatment of OC cells with the individual drugs alone and combination in a dose-dependent manner, the highest proportion of cell apoptosis was observed in the high-dose group treated with SB-HD and DDP combination in both SKOV3 and OVCAR3 cells (Fig. 2F-I).

SB-HD and DDP synergistically inhibited the migration and invasion of OC cells

Wound healing assay was used to detect the SB-HD and DDP synergistically inhibitory effect on the lateral migration capacities of OC cells, as shown in Fig. 3A-B, SB-HD alone and in combination with DDP effectively prevented wound healing. To further explore the effect of combination treatment on cell vertical migration and invasion, we performed transwell assay. The results showed that SKOV3 and OVCAR3 cells without any treatment could move through the upper well to the lower chamber. Meanwhile, we found that cells treated with SB-HD and DDP effectively reduced the percent of cell migration and cell invasion in a dose-dependent manner comparing with the treatment of DDP alone (Fig. 3C-H).

Inhibition of xenografted tumors in vivo by combination treatment

The effect of the combination treatment on SKOV3 tumor growth was assessed in vivo. After 2 weeks, the mice were killed and the tumor was exfoliated, the weight and volume of the tumor were recorded and photographed. Compared with control and the individual drugs alone, combination treatment significantly inhibited tumor growth and reduced the size of tumors (Fig. 4A-E). Compared with control group, the body weight and spleen index of DDP group mice were significantly reduced, while the kidney index was significantly increased and no significant change in liver index, combination treatment has a significant improvement in these changes (Fig. 4F-G). By HE staining, the heart, liver, spleen, lungs, and kidneys histology morphology of mice were not significantly different among groups (Fig. 4H). Compared with control group, levels of serum ALT, AST, BUN and Cre significantly increased in DDP group, and combination treatment has a significant improvement effect (Fig. 4I). In short, the combination treatment produced no observable toxic effects and has a certain detoxifying effect. Furthermore, consistent with loose arrangement of tumor tissue, the number of Ki-67-positive cells was significantly decreased in SB-HD+DDP group (Fig. 4J).

Combination treatment induced OC cells oxidative stress, and increased the expression of NRF2 and HO-1 in tumor tissues

In order to explore the possible mechanisms for the synergistic effects of SB-HD and DDP, we first incubated the cells with the JC-1 probe to detect MMP, SB-HD alone and in combination with DDP resulted in obvious decrease of MMP, and the latter decreases more significantly in both SKOV3 and OVCAR3 cells (Fig. 5A-D). So was ROS levels in both SKOV3 and OVCAR3 cells, but the former SB-HD alone may decrease a bit more (Fig. 5E-H). Then, we examined the ATP content and antioxidant enzyme SOD activity in co-treated cells. Combination treatment significantly decreased the ATP content and increased SOD activity comparing with the treatment of DDP alone (Fig. 5I-J). Subsequently, we stained tumor tissues with the primary antibody NRF2 and HO-1, which are oxidative stress-associated important molecules, as shown Fig. 5K, combination treatment markedly induced their expression.

Combination treatment reduced the expression of FTH1 in OC cells and tumor tissues through autophagy

Based on these results, oxidative stress may play an important role in cancer development. In addition, our team's previous results have shown that ferritinophagy plays an important role in SB-HD induced OC cell death.

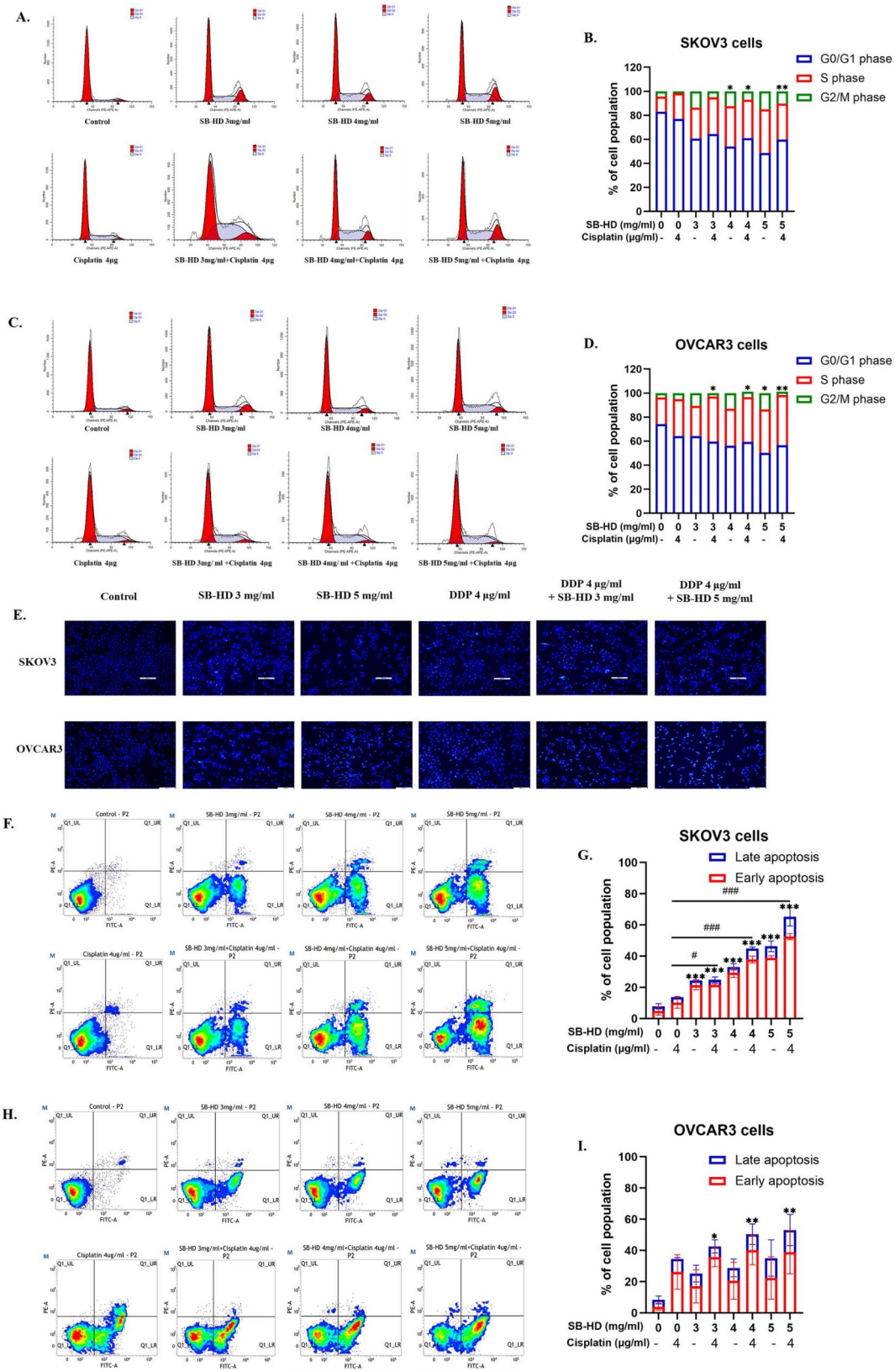


Fig. 2 SB-HD alone and in combination with DDP promoted cell cycle arrest and apoptosis. (A–D) Distribution analysis of cell cycle of SKOV3 and OVCAR3 cells after treatment. (E) Detection of cell apoptosis by Hoechst 33,342 staining assay. (F–I) Quantitative analysis of cell apoptosis by Annexin V/PI double staining assay and flow-cytometry calculation (* $p < 0.05$, ** $p < 0.01$, *** $p < 0.001$ vs control; # $p < 0.05$, ## $p < 0.01$, ### $p < 0.001$ vs DDP; $n = 3$)

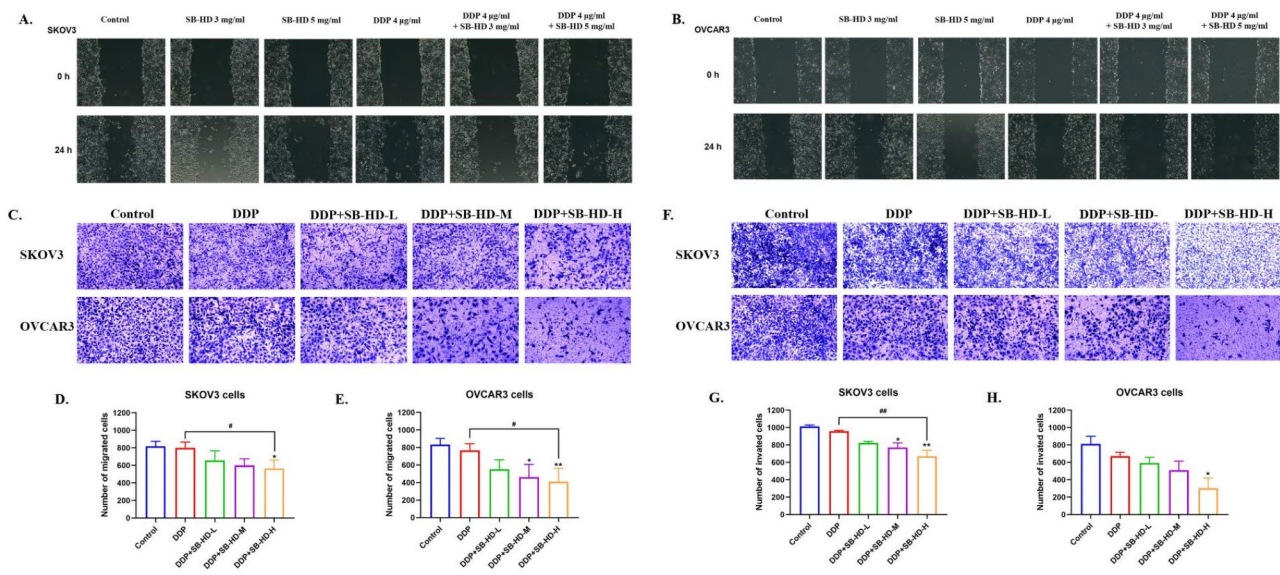


Fig. 3 Inhibition of cell migration and invasion by SB-HD and DDP. (A–B) The effects of treatment for 24 h on horizontal migration of SKOV3 and OVCAR3 cells measured by wound healing assay. (C–H) The effects of treatment on vertical migration and invasion of SKOV3 and OVCAR3 cells measured by Transwell™ assay (* $p < 0.05$, ** $p < 0.01$, *** $p < 0.001$ vs control; # $p < 0.05$, ## $p < 0.01$, ### $p < 0.001$ vs DDP; $n = 3$)

Therefore, we speculate whether SB-HD enhances the sensitivity of OC to DDP chemotherapy based on oxidative stress and ferritin autophagic degradation. Here, by Western blotting experiments, we measured oxidative stress and autophagy associated proteins: NRF2, HO-1, p62, ATG5, LC3 and FTH1. We found that the combination of SB-HD and DDP significantly increased the expression of NRF2, HO-1, ATG5 and LC3, and decreased the expression of p62 and FTH1 both in OC cells and tumor tissue of mice (Fig. 6A–E). It demonstrated that combination treatment promoted FTH1 degradation in OC cells and tumor tissues through autophagy.

Inhibitors 3-MA and Fer-1 reversed FTH1 autophagy degradation of OC cells under combination treatment

To further explore the underlying mechanisms of SB-HD enhancing the DDP chemosensitivity of OC, on the basis treated of the combination of SB-HD and DDP, three inhibitors Fer-1, ZnPP and 3-MA were used to treat SKOV3 and OVCAR3 cells. The results showed that inhibitors 3-MA and Fer-1 effectively reversed the expression changes of the target proteins, but not inhibitor ZnPP. Fer-1 can obviously reverse the expression of NRF2, HO-1, and FTH1 in this signaling pathway (Fig. 6F–H). Taken together, we concluded that SB-HD synergistically promotes the inhibitory effect of DDP on OC by inducing NRF2-FTH1 autophagic degradation pathway.

Clinical prognostic value of target genes of combination treatment in OC

Through the GEPIA database, we directly got the results of the correlation between the target proteins and OC, and the color deepened with the increase of the correlation value, as shown in Fig. S1. From the results of the heat map, we can intuitively and clearly observe that OC is closely related to NRF2 (6.9), HO-1 (6.1), p62 (7.8), ATG5 (3.7), LC3 (6.1) and FTH1 (11.6), among which FTH1 has the highest correlation score. In order to find their specific relationship with OC, more comprehensive analysis was performed to understand the role of target genes in OC.

As shown in Fig. 7A, we performed an analysis of gene expression profiles in OC samples and normal tissues using GEPIA. It was found that the expression levels of NRF2 ($p < 0.05$), HO-1 ($p < 0.05$) and LC3 in OC tissues were lower than those in normal tissues, while the expression levels of FTH1 ($p < 0.05$), p62 and ATG5 were higher. Moreover, we found that the expression range of six target genes was the widest in the clinical stage III of OC. The expression of NRF2, HO-1, ATG5 and NRF2 was decreased in clinical stage III and IV of OC, NRF2 ($p < 0.001$) was the most significantly decreased, but the expression of p62, LC3 and FTH1 in clinical stages of OC had no difference, as shown in Fig. 7B. To assess the prognostic value of the target genes in OC, we plotted specific survival curves using the TCGA database. Kaplan–Meier curve analysis revealed a correlation between high expression of NRF2 ($p < 0.05$) and prolonged progression free survival (PFS) in OC patients. Conversely, low expression of p62 ($p < 0.05$) was significantly associated

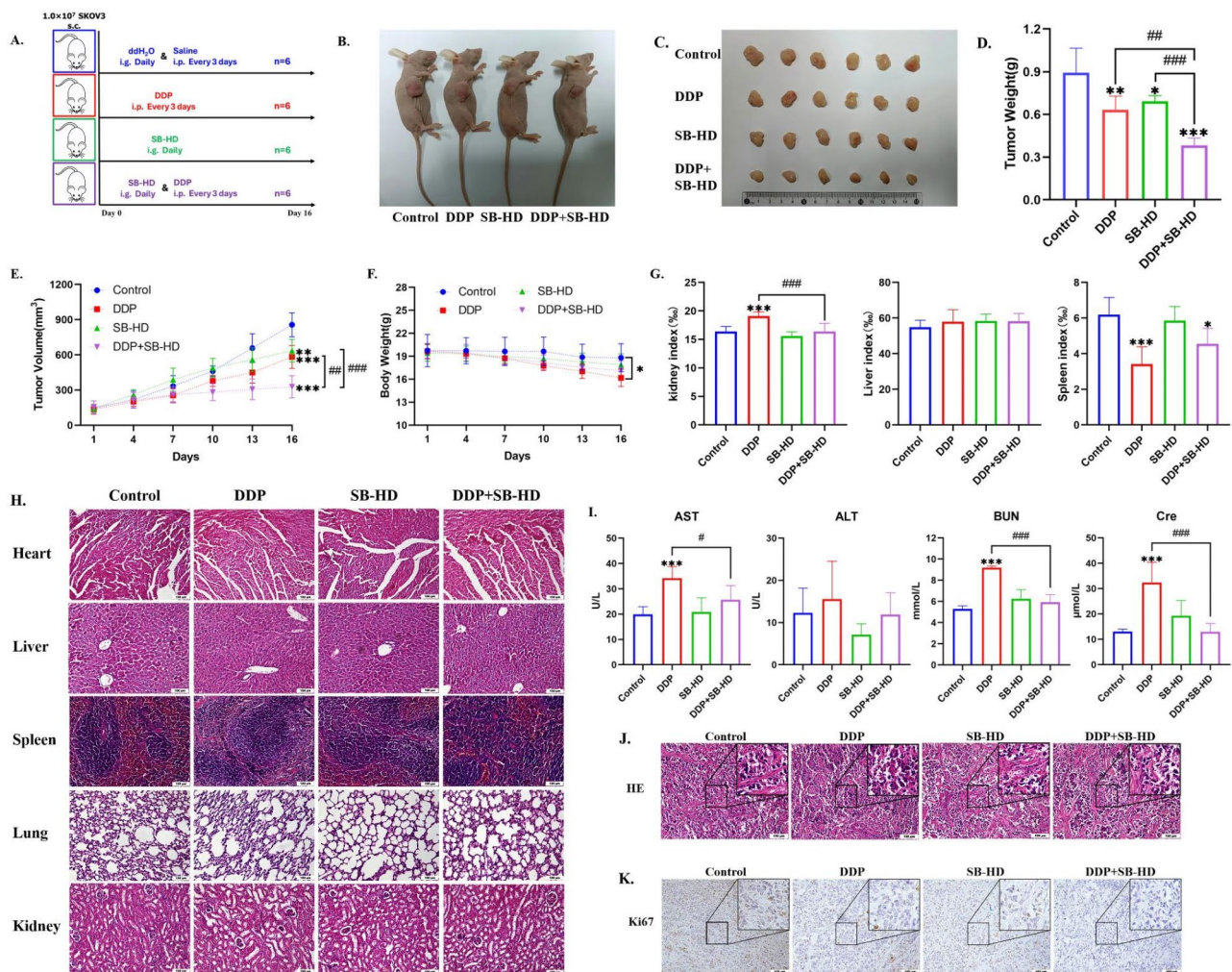


Fig. 4 Combination treatment inhibited xenograft tumor growth in vivo. (A) Experimental set-up. (B) Representative image of xenografted tumors in mice. (C) Anatomical view of mouse tumors. (D) The average weight of the tumors. (E) Tumor growth curve. (F) Body weight curves of mice. (G) Kidney index, Liver index and Spleen index. (H) HE staining of the heart, liver, spleen, lung and kidney (scale bar = 100 μm). (I) AST, ALT, BUN, and Cre levels of mice after treatment. (J) HE staining of tumors (scale bar = 100 μm). (K) IHC analysis of Ki67 expression in tumor tissues (* $p < 0.05$, ** $p < 0.01$, *** $p < 0.001$ vs control; # $p < 0.05$, ## $p < 0.01$, ### $p < 0.001$ vs DDP; $n = 3-6$)

with prolonged PFS. However, the expression of ATG5, LC3, FTH1 and HO-1 showed no significant correlation with PFS in OC patients (Fig. 7C). Next, we used the GEPIA database platform to further explore the genetic alterations of target genes in OC patients. The 1691 ovarian serous cystadenocarcinoma tissue samples from 1674 patients included in the TCGA3 data set were retrieved, the results showed that the mutation rates of the target genes NRF2, HO-1, p62, ATG5, LC3 and FTH1 ranged from 1 to 5%, and the mutation types were mainly amplified. The results are shown in Fig. 7D. Among them, NRF2 mutation rate was the highest, the order of the other mutations rate is: LC3 > p62 and ATG5 > HO-1 > FTH1, moreover, p62 and ATG5 were prone to deletion mutations.

Finally, we conducted Pearson correlation coefficient analysis to assess the correlation of these six core genes,

a visualized heat map was drawn, as shown in Fig. 7E. The correlation coefficient ranges from 0.0065 (NRF2 vs. LC3) To 0.5 (p62 and FTH1). According to whether the value was statistically significant ($p < 0.05$), we found that NRF2 was directly correlated with HO-1, p62 was directly correlated with ATG5, HO-1 was directly correlated with p62 (Already described correlation is omitted), p62 was directly correlated with ATG5 and LC3, LC3 was directly correlated with FTH1, respectively. The above results indicate that there are close interactions among the target genes in OC, which further suggests that the target genes can participate in the occurrence and development of OC in an interactive manner.

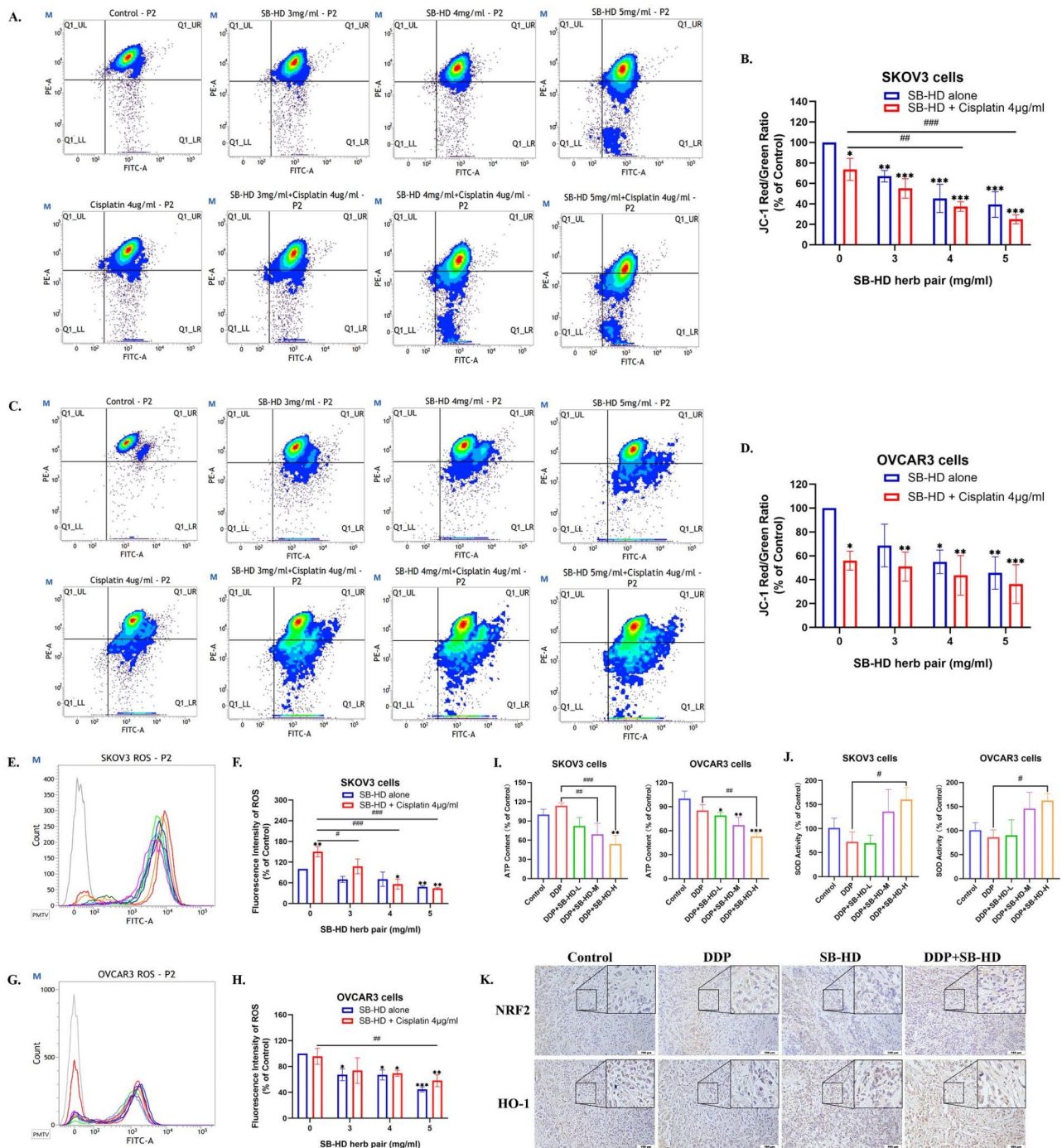


Fig. 5 Combination treatment induced oxidative stress. **(A–D)** The MMP and **(E–H)** ROS levels of OC cells treated with SB-HD alone and in combination with DDP. **(I)** The ATP content and **(J)** SOD activity of OC cells treated with SB-HD in combination with DDP. **(K)** IHC analysis of NRF2 and HO-1 expression in tumor tissues (* $p < 0.05$, ** $p < 0.01$, *** $p < 0.001$ vs control; # $p < 0.05$, ## $p < 0.01$, ### $p < 0.001$ vs DDP; $n = 3$)

Discussion

In recent years, studies have shown that SB and HD are commonly used in various cancers such as prostate cancer, ovarian cancer, liver cancer, gastric cancer, and colorectal cancer, etc [18–23]. The mechanism mainly includes multiple signaling pathways such as PI3K/

Akt/mTOR, AMPK, P53, etc., which inhibit the proliferation, migration and invasion of tumor cells, promote tumor cell apoptosis, and thus achieve the goal of inhibiting tumor growth [18–23]. In addition, they can also enhance the body’s immune function and enhance the body’s resistance to tumors [24]. As a natural medicine,

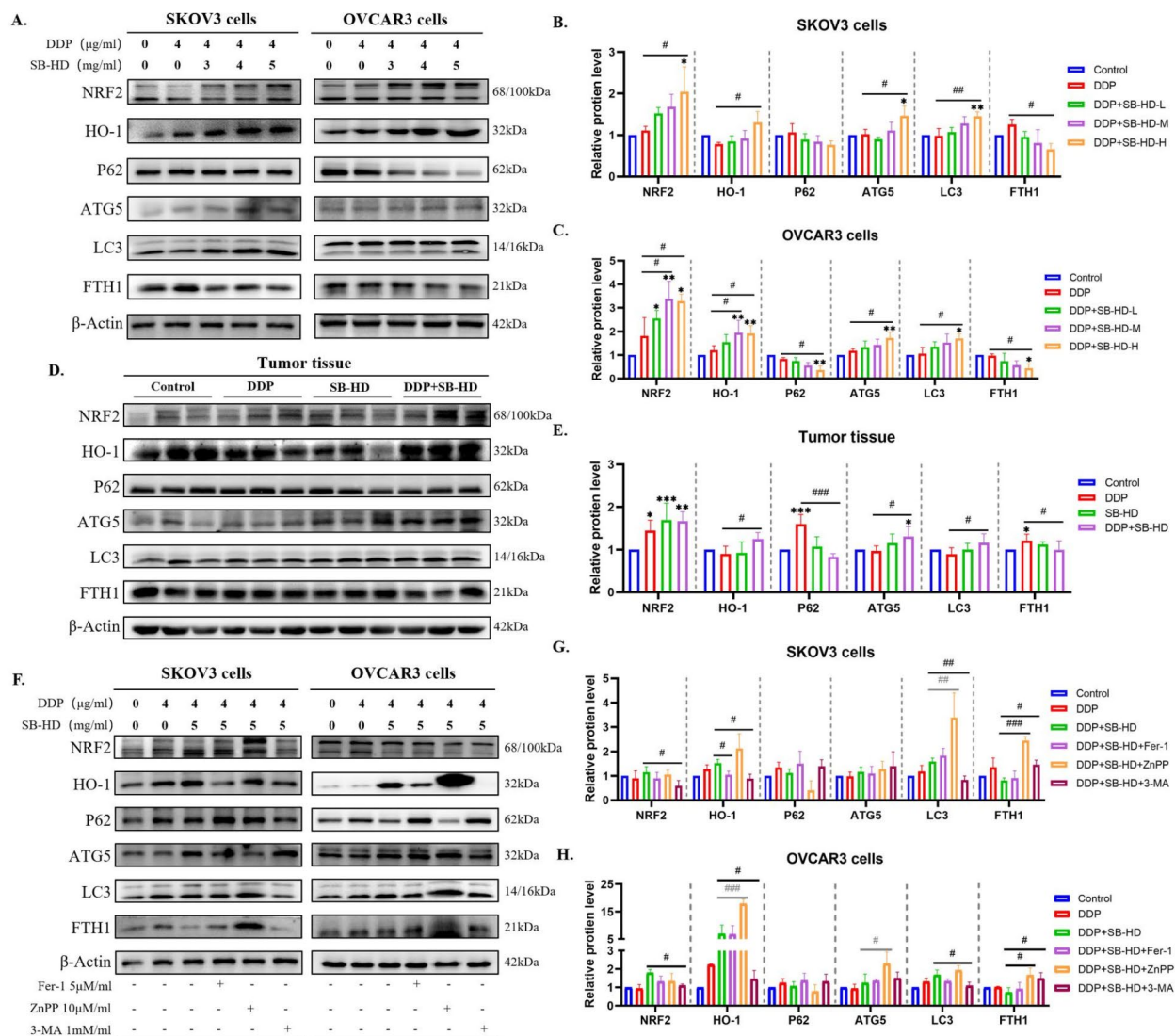


Fig. 6 Combination treatment promoted FTH1 autophagic degradation in OC cells and tumor tissues. (A–E) Western blotting analysis and quantification of the expression of NRF2, HO-1, p62, ATG5, LC3 and FTH1 in OC cells and tumor tissues under different treatments. (F–H) Western blotting analysis and quantification of associated proteins in OC cells under different drugs treatments with inhibitors Fer-1, ZnPP or 3-MA (* $p < 0.05$, ** $p < 0.01$, *** $p < 0.001$ vs control; # $p < 0.05$, ## $p < 0.01$, ### $p < 0.001$ vs DDP; $n = 3$)

they have the potential to be combined with current chemotherapy to improve the therapeutic effect of existing drugs and exhibit good application prospects. In this study, we first evaluate the synergistic effects of SB-HD and DDP on OC, it was found combination treatment obviously inhibited the colony formation, promoted cell cycle arrest and cell apoptosis, inhibited the proliferation of OC cells in vitro and in vivo, and explored its possible mechanisms which is through modulating oxidative stress via NRF2-FTH1 autophagic degradation pathway. The schematic diagram is shown in Fig. 8.

As is well known, the clinical treatment of OC often uses paclitaxel combined with such as carboplatin or DDP which is a combination chemotherapy regimen at

present [25]. Although the short-term effect in preventing tumor growth, killing or eliminating tumor cells is optimistic, it cannot be ignored the adverse reactions and drug resistance. Like DDP, it is one of the most effective anticancer drugs and is commonly used to treat advanced OC, while it may occur kidney injury, liver injury, digestive tract injury, some potential neurotoxicity and muscle toxicity caused by long-term use or at high dose [26]. Therefore, in our experiment, we evaluated organ damage in the heart, liver, spleen, lungs, and kidneys of mice, examined the liver, kidney and spleen indices, our results proved that SB-HD reduces the effect of DDP on the kidney damage in OC bearing mice, and has a slight immune protective effect by increasing spleen indices. We also

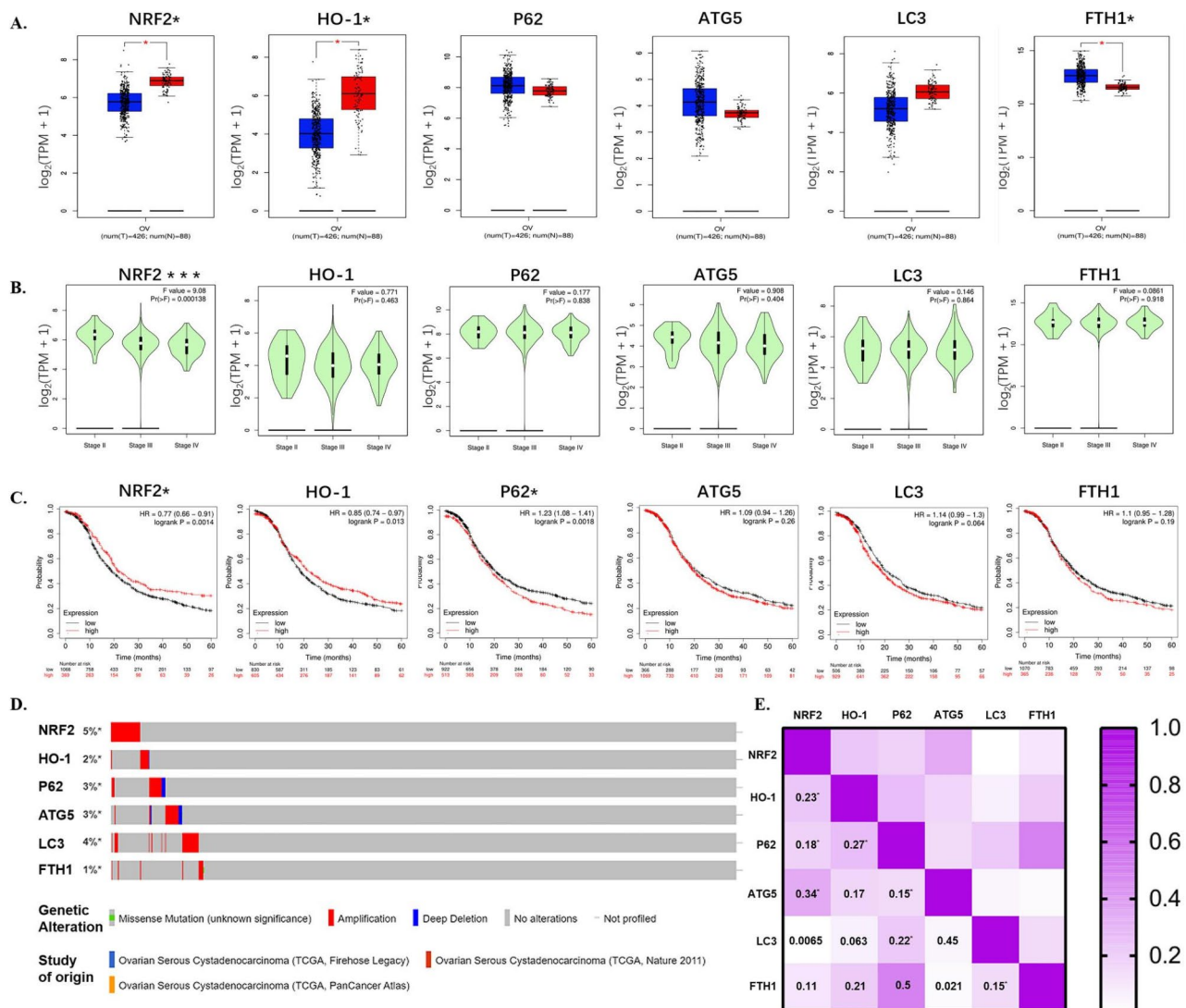


Fig. 7 Validation of clinical prognostic value of combination treatment target genes expression in OC by bioinformatics analysis. **(A)** mRNA expression of target genes in OC tissues compared to normal tissues, indicated by asterisks. (Blue: OC samples; Red: normal tissues.) **(B)** The relationship between mRNA expression of target genes and the clinical stage of OC. **(C)** Kaplan–Meier survival analysis of target genes of OC patients, showing high and low expression groups. **(D)** Genetic variation analysis of target genes in OC patients. **(E)** The visual heat map of Pearson correlation analysis among target genes. Correlation coefficient between 0 and 1, the color indicates the strength of the correlation. Direct correlation indicated by asterisks

carried out measuring the possible hepatotoxicity and nephrotoxicity of the combination of the two drugs by detecting biochemical indicators ALT, AST, BUN and Cre, which shows that combination treatment markedly reduced the levels of serum ALT, AST, BUN and Cre compared to the DDP alone. Compared with the weight loss of mice in the DDP treatment group, the combination treatment did not affect the weight change, indicating that both SB-HD monotherapy and combination therapy have good safety.

Cancer metastasis is one of the biological characteristics of malignant tumors, which leads to the failure of surgery, radiotherapy and chemotherapy, as well as the death of patients [27]. Cancer cells interact with host cells

and affect their microenvironment for survival. Epithelial-mesenchymal transition (EMT) is a process in which tumor cells acquire the ability of migration and invasion due to the loss of epithelial phenotype and the dramatic change of epithelial layer [28]. This process is the main step to promote the metastasis of tumor cells. Here, compared with other types of solid tumors, OC is more likely to metastasize. OC cells mostly grow on the surface of the ovary in the abdominal cavity and are easy to adhere to adjacent tissues. In addition, OC is often accompanied by cancerous ascites, so intra-abdominal contact implantation is the most common mode of metastasis in patients with OC. Most OC patients die from advanced diseases, accompanied by peritoneal metastasis and

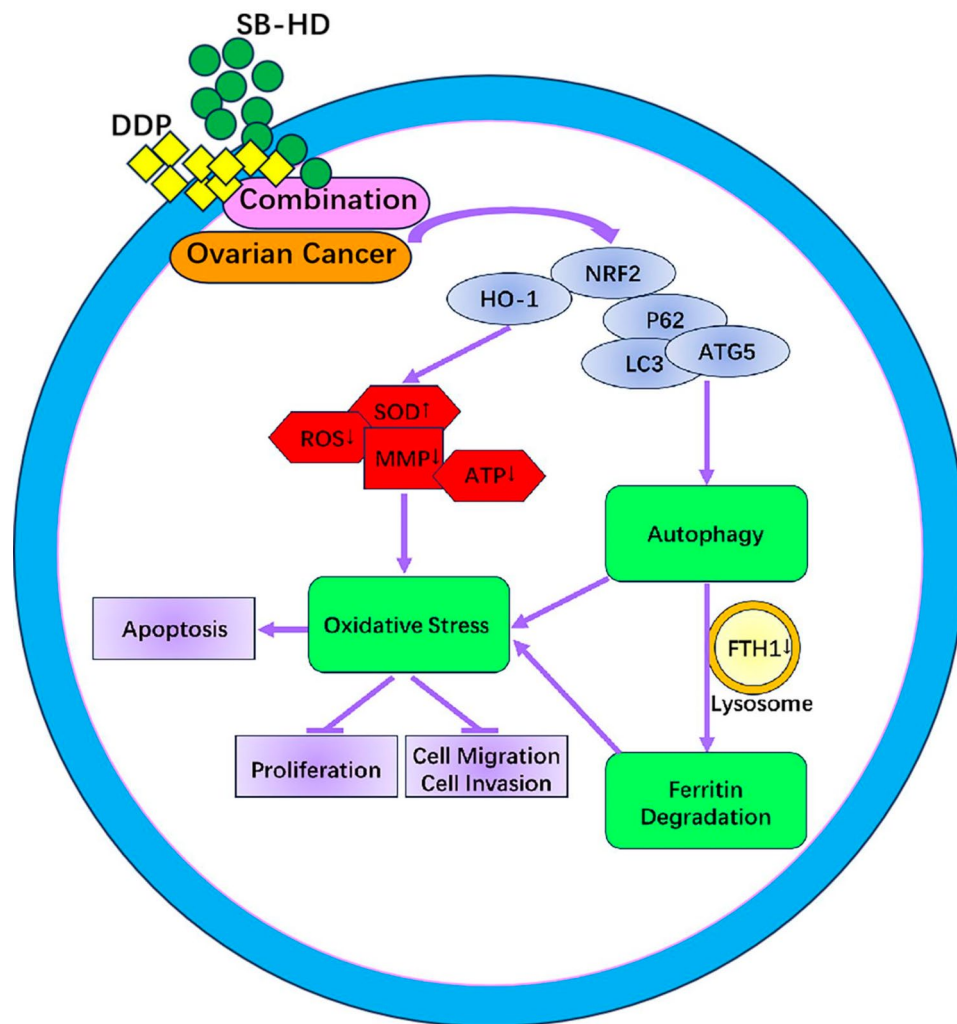


Fig. 8 Schematic drawing of the potential molecular mechanism of SB-HD enhancing DDP chemotherapy sensitivity in OC

poor prognosis. Therefore, in this study, we investigated the inhibiting effects of SB-HD alone or in combination with DDP on migration and invasion of OC SKOV3 and OVCAR3 cells, and our results confirmed inhibiting the migration and invasion role in a dose-dependent manner in vitro by wound healing assay, transwell cell migration assay and transwell cell invasion assay. Moreover, it is noteworthy that the expression of p62 is significantly elevated in tumor tissues treated with DDP alone in western blot analysis. It has been reported that p62 as an oncotarget mediates cisplatin resistance and high p62 cytoplasmic expression was shown to be associated with poor prognosis [29, 30]. Besides, Lu et al. found that p62 knockout inhibits migration and invasion of hepatocellular carcinoma [31], high expression of p62-induced EMT with the upregulation of Snail, vimentin, N-cadherin, and downregulation of E-cadherin, which might play a vital role in maintaining the mitochondrial function of intrahepatic cholangiocarcinoma (ICC) [32]. In our study,

DDP treatment induced p62 expression was suppressed by drug combination treatment, suggested that tumor tissue cells may be inhibited gradually developing DDP resistance and EMT. In subsequent research, we may conduct an animal model of ascites metastasis of OC to focus on cancer metastasis.

Autophagy is an intracellular metabolic process, which may be caused by oxidative stress plays an important role in the development of tumors, participates in the energy metabolism and material metabolism of tumor cells, changes MMP and related metabolites including ATP, ROS, SOD and so on, as well as affect the changes of tumor growth microenvironment [33, 34]. First of all, mitochondria are the energy center and regulator of cells. The decline in MMP is a landmark event in the early stages of cell apoptosis. In our study, SB-HD increased the proportion of early and late apoptosis in SKOV3 and OVCAR3 cells, and decreased MMP compared with Control. Compared with DDP alone, the combination

treatment significantly increased the proportion of apoptosis and further promoted the decrease of MMP. In addition, ATP is an intracellular energy molecule and an important regulator of autophagy, and it can also regulate the immune response in the tumor microenvironment, enhance the body's immune surveillance and elimination of tumors [35]. So, we examined the changes of ATP in SB-HD combined with DDP subsequently, and found that combination treatment could reduce ATP levels in SKOV3 and OVCAR3 cells. It is known that the levels of ATP are closely related to the degree of autophagy in tumor cells. When tumor cells are in a low energy state, the level of ATP decreases, which can activate AMPK signaling pathway and promote the initiation of autophagy [36]. As expected, our Western blotting results showed autophagy-associated proteins to be induced in the combination treatment.

Several studies have reported that mitochondria are the main sites of oxygen free radicals in cells, and also an important target of oxidative stress. Excessive levels of oxygen free radicals can lead to mitochondrial dysfunction and DNA oxidative damage. ROS can play a dual role in anti-tumor by affecting mitochondrial function, the effect depends on the levels of ROS and the state of the cells [37, 38]. In this study, we found that ROS content in cells treated with SB-HD extract alone and combination treatment showed a significant downward trend, and there was no significant difference between SB-HD extract alone and combination treatment. According to the existing research, ROS plays an important role in promoting cell mitosis, which is indispensable to induce cell proliferation. When ROS accumulates in cells, it can induce apoptosis due to oxidative stress, but it is less toxic to the corresponding normal cells. When ROS is at a low level, the cells will be in a state of proliferation inhibition, but the corresponding normal cells are less sensitive to it. The difference of drug sensitivity between tumor cells and normal cells may be due to the high levels of ROS expression in tumor cells themselves. Our results suggest that combination treatment reduce the levels of ROS in OC cells, which lead to cell cycle inhibition.

From a biological function, SOD is a kind of metallo-proteinase in mitochondria, which is a powerful oxygen free radical scavenger. Its main function is to remove superoxide anion (O_2^-) in cells and prevent the occurrence of oxidative damage. It has been reported that SB has immunomodulatory effect and anti-lipid peroxidation effect, which can scavenge oxygen negative free radicals and improve the activity of SOD, and its antioxidant effect has been widely accepted. HD has also been found to increase the activity of SOD in gastric tissue, reduce the content of MDA, and have a protective effect on gastric ulcer and other gastrointestinal membrane damage. Therefore, we speculated that SB-HD assisted DDP

to down-regulate ROS in OC, SOD activity may play an important role. Subsequently, we detected the SOD activity in each group of cells treated with different drugs, and found that combination treatment increased the activity of SOD, which proved our inference. In tumor cells, SOD activity is usually low, and studies have shown that the occurrence of some cancers is related to the decline of SOD levels in vivo. By increasing the levels of SOD, it is expected to provide new ideas for cancer prevention and treatment.

Ferroptosis is a new way of cell death, which is different from the traditional ways of cell death such as necrosis and apoptosis, and was first proposed in 2012 [39]. Recent studies have pointed out that ferroptosis may be autophagy-dependent, because the response to ferroptosis activators can lead to the accumulation of autophagosomes, and the components of autophagy mechanism contribute to the occurrence of ferroptosis [14]. In addition, FTH1 encodes a ferritin heavy chain, the autophagic degradation of FTH1 can increase oxidative stress and the level of Fe^{3+} in cells, making cells more sensitive to ferroptosis [40]. At the same time, ferroptosis depends on the accumulation of intracellular iron and ROS [41, 42]. Iron-dependent lipid peroxidation is the main feature of cell ferroptosis, and the damage of cell membrane caused by lipid peroxides is an important reason for ferroptosis [41, 42]. Besides, nuclear receptor coactivator 4 (NCOA4) is a selective receptor that maintains iron homeostasis by binding to ferritin, transporting it to the lysosome, and promoting autophagy degradation, and is considered as an important regulator of ferroptosis [43, 44]. It has been reported that a decrease in intracellular Fe^{2+} /oxidative stress response and an increase in glutathione level are accompanied by an decrease in NCOA4 expression, revealed that the level of oxidative stress is closely related to NCOA4 [44]. In our study, we have preliminarily found an increase in this protein expression by combination treatment, this may also imply an increase in oxidative stress. According to the results, combination treatment reduces the level of intracellular ROS, we speculate that although SB-HD can enhance the sensitivity of DDP chemotherapy in OC by regulating oxidative stress and activating autophagy, but it is may not further promote the occurrence of cell ferroptosis. Because the high activity of SOD enzyme generally indicates that there are too many free radicals in the body. ROS is a series of active oxygen free radicals produced by cells in the process of metabolism, which is essentially a chemical substance with unpaired electrons and has a strong ability to compete for electrons. A large amount of ROS will lead to the decrease of MMP and ATP content, then promote cell apoptosis and the destruction of mitochondrial homeostasis. Mitochondria are important mediators of cellular metabolism, producers and targets of ROS. The

disruption of mitochondrial homeostasis leads to the decrease of ROS follow-up production, and along with the increase of SOD activity further reduces ROS levels, meanwhile, autophagy also acts as a ROS scavenger in cancer cells. To sum up, the dynamic changes mentioned above may regulate OC cells in a state of oxidative stress, which is a joint effect by regulating autophagy, affecting MMP, ROS production, ATP content and SOD activity.

NRF2/HO-1 pathway plays an important role in the occurrence and regulation of oxidative stress and inflammatory response [45–47]. Some studies suggest that NRF2/HO-1 is involved in regulating autophagy and cell apoptosis [48–51]. In the preliminary research of our team, NRF2 and HO-1 were significantly increased in the OC cells treated with SB-HD alone by proteome and transcriptome analysis, simultaneously were validated by Western blotting and quantitative PCR (qPCR) experiments with or without inhibitors Fer-1, ZnPP and 3-MA. Research has illustrated that ferritinophagy may be the key reason SB-HD induces ferroptosis in OC cells and thus exert anti-tumor effects. In this study, we first found NRF2 and HO-1 in the tumor tissue was significantly increased by IHC stained, and also detected the combination treatment significantly increased the expression of NRF2 and HO-1 both in OC cells and tumor tissue of mice by Western blotting experiments. Moreover, we found that combination treatment reduced the expression of FTH1 in OC cells and tumor tissues through autophagy. Next, to further clarify the molecular mechanism, three inhibitors of Fer-1, ZnPP and 3-MA were used to extract cellular proteins on the basis of the combination treatment in this part of the experiment. 3-MA can effectively reverse the expression changes of the target proteins. Fer-1 can obviously reverse the expression of NRF2, HO-1, and FTH1 in this signaling pathway. Therefore, we conclude that the mechanism by which SB-HD increases sensitivity to DDP chemotherapy in OC may be primarily associated with ferroptosis related oxidative stress and autophagic degradation of ferritin. Interestingly, we also found that HO-1 decreased in SKOV3 cells after the use of the inhibitor Fer-1, and increased in OVCAR3 cells after the use of the inhibitor ZnPP. As Fer-1 is a synthetic antioxidant, it mainly prevents the damage of membrane lipids through a reductive mechanism, thereby inhibiting cell death. Therefore, we speculated that the addition of Fer-1 to SKOV3 cells may compensate for part of the antioxidant activity of the cells originally produced by HO-1, which result in decreasing HO-1 expression. However, ZnPP is a competitive inhibitor of HO-1 which has anticancer activity. The concept of competitive inhibitor refers to the inhibitor that produces competitive inhibition, which usually has structural similarity with the substrate of the inhibited enzyme, and can compete with the substrate for the binding site on the

enzyme molecule, thus producing reversible inhibition of enzyme activity. In this study, the inhibitor ZnPP was added to inactivate HO-1, which may destroy the important physiological and pathological functions of HO-1 involved in regulation, and then trigger more HO-1 expression in positive feedback, so the detected HO-1 expression level increased significantly.

Finally, due to the complex clinical features of OC, we also analyzed the key target genes by bioinformatics utilizing online large databases, hoping to return the problems in clinical practice to the clinical cases for further analysis and exploration, in order to clarify the correlation between target genes and OC, the expression differences between healthy people and patients, the expression level in clinical stages and the prognosis. We found that the abnormal expression levels of NRF2 and FTH1 mRNA showed high prognostic value. The other four target genes of this signaling pathway HO-1, p62, ATG5 and LC3, also play an important role in the development of OC, either individually or by interacting with NRF2 and FTH1. We conclude that NRF2 and FTH1 may become potential biomarkers for individualized prediction and treatment of OC. It may provide a reference for the potential study of DDP combined with other herb drugs to enhance the chemosensitivity of OC.

Conclusion

In conclusion, our present study demonstrated that SB-HD combined with DDP have synergistic enhancing efficiency and reducing toxicity effects in the treatment of OC. Mechanistically, SB-HD promote the proliferation and metastasis inhibition of DDP on OC through modulating oxidative stress via NRF2-FTH1 ferritin autophagic degradation pathway, thus enhance the chemosensitivity of OC to DDP. SB-HD may be used as a potential DDP combination drug to provide new ideas and therapeutic strategy for the clinical treatment of OC, which has potential clinical applications in reducing the side effects of cancer chemotherapy.

Abbreviations

ALT	Alanine aminotransferase
AST	Aspartate aminotransferase
ATG5	Autophagy related 5
ATP	Adenosine triphosphate
BUN	Blood urea nitrogen
CCK-8	Cell counting kit-8
Cre	Creatinine
Fer-1	Ferrostatin-1
FTH1	Ferritin heavy chain 1
HE	Hematoxylin-eosin
HO-1/HMOX1	Heme oxygenase-1
IHC	Immunohistochemistry
LC3/MAP1LC3A	Microtubule associated protein 1 light chain 3 alpha
MMP	Mitochondrial membrane potential
NRF2/NFE2L2	Nuclear factor-erythroid 2-related factor 2
PFS	Progression free survival
p62/SQSTM1	Sequestosome-1
qPCR	Quantitative PCR

ROS	Reactive oxidative species
SOD	Superoxide dismutase
ZnPP	Zinc protoporphyrin
3-MA	Methyladenine

Supplementary Information

The online version contains supplementary material available at <https://doi.org/10.1186/s13048-024-01570-6>.

Supplementary Material 1

Acknowledgements

Not applicable.

Author contributions

Xue Sui: Conceptualization, Investigation, Methodology, Validation, Data curation, Formal analysis, Visualization, Resources, Writing—original draft, Writing—review & editing. Bingqing Gao: Investigation, Methodology, Validation, Data curation, Formal analysis, Visualization. Liu Zhang: Validation, Data curation, Formal analysis. Yanmin Wang: Conceptualization, Methodology, Visualization. Junnan Ma: Investigation, Methodology, Formal analysis. Xingchen Wu: Data curation, Formal analysis. Chenyu Zhou: Data curation, Formal analysis. Min Liu: Conceptualization, Methodology, Supervision, Visualization, Resources, Writing—review & editing. Lin Zhang: Project administration, Funding acquisition, Conceptualization, Methodology, Supervision, Resources, Writing—review & editing. All authors reviewed the manuscript.

Data availability

No datasets were generated or analysed during the current study.

Declarations

Ethics approval and consent to participate

All experimental protocols in the current study were performed in strict accordance with the institutional guidelines and approved by the Animal Ethical Committee of Dalian Medical University.

Consent for publication

Not applicable.

Competing interests

The authors declare no competing interests.

Author details

¹Institute (College) of Integrative Medicine, Dalian Medical University, Dalian 116044, China

²School of Pharmacy, Anhui Xinhua University, Hefei 230088, China

³Department of Dermatology, Dalian Lvshunkou District Hospital of Traditional Chinese Medicine, Dalian 116041, China

⁴Advanced Institute for Medical Sciences, Dalian Medical University, Dalian 116044, China

Received: 19 June 2024 / Accepted: 30 November 2024

Published online: 19 December 2024

References

- Sung H, Ferlay J, Siegel RL, Laversanne M, Soerjomataram I, Jemal A, et al. Global Cancer statistics 2020: GLOBOCAN estimates of incidence and Mortality Worldwide for 36 cancers in 185 countries. *CA Cancer J Clin*. 2021;71:209–49.
- Lheureux S, Braunstein M, Oza AM. Epithelial ovarian cancer: evolution of management in the era of precision medicine. *Cancer J Clin*. 2019;69.
- Ghosh S. Cisplatin: the first metal based anticancer drug. *Bioorg Chem*. 2019;88:102925.
- Zoń A, Bednarek I. Cisplatin in ovarian Cancer treatment—known limitations in Therapy Force New solutions. *IJMS*. 2023;24:7585.
- Zhang Y, Liang Y, He C. Anticancer activities and mechanisms of heat-clearing and detoxifying traditional Chinese herbal medicine. *Chin Med*. 2017;12:20.
- Zhang L, Ren B, Zhang J, Liu L, Liu J, Jiang G, et al. Anti-tumor Effect of *Scutellaria Barbata* D. Don extracts on ovarian Cancer and its phytochemicals characterisation. *J Ethnopharmacol*. 2017;206:184–92.
- Zhang L, Zhang J, Qi B, Jiang G, Liu J, Zhang P, et al. The anti-tumor effect and bioactive phytochemicals of *Hedyotis diffusa* willd on ovarian cancer cells. *J Ethnopharmacol*. 2016;192:132–9.
- Glick D, Barth S, Macleod KF. Autophagy: cellular and molecular mechanisms. *J Pathol*. 2010;221.
- Chiang SK, Chen SE, Chang LC. The role of HO-1 and its crosstalk with oxidative stress in Cancer Cell Survival. *Cells*. 2021;10:2401.
- Das S, Shukla N, Singh SS, Kushwaha S, Shrivastava R. Mechanism of interaction between autophagy and apoptosis in cancer. *Apoptosis*. 2021;26:512–33.
- Liu S, Pi J, Zhang Q. Signal amplification in the KEAP1-NRF2-ARE antioxidant response pathway. *Redox Biol*. 2022;54:102389.
- Hybertson BM, Gao B, Bose SK, Mccord JM. Oxidative stress in health and disease: the therapeutic potential of Nrf2 activation. *Mol Aspects Med*. 2011;32:234–46.
- Furfaro AL, Traverso N, Domenicotti CM, Piras S, Moretta L, Marinari U, et al. The Nrf2/HO-1 axis in cancer cell growth and chemoresistance. Hindawi Publishing Corporation; 2016.
- Zhou B, Liu J, Kang R, Klionsky DJ, Kroemer G, Tang D. Ferroptosis is a type of autophagy-dependent cell death. *Sem Cancer Biol*. 2020;66:89–100.
- Shi Z, Yuan H, Cao L, Lin Y. AKT1 participates in ferroptosis vulnerability by driving autophagic degradation of FTH1 in cisplatin-resistant ovarian cancer. *Biochem Cell Biol*. 2023;101:422–31.
- Santana-Codina N, Del Rey MQ, Kapner KS, Zhang H, Gikandi A, Malcolm C, et al. NCOA4-Mediated ferritinophagy is a pancreatic Cancer dependency via maintenance of Iron Bioavailability for Iron–sulfur cluster proteins. *Cancer Discov*. 2022;12:2180–97.
- Qu C, Dai E, Lai T, Cao G, Liu J, Kang R, et al. Itaconic acid induces ferroptosis by activating ferritinophagy. *Biochem Biophys Res Commun*. 2021;583:56–62.
- Sheng D, Zhao B, Zhu W, Wang T, Peng Y. *Scutellaria Barbata* D. Don (SBD) extracts suppressed tumor growth, metastasis and angiogenesis in prostate cancer via PI3K/Akt pathway. *BMC Complement Med Ther*. 2022;22:1–16.
- Peng J. *Scutellaria Barbata* D. Don induces G1/S arrest via modulation of p53 and akt pathways in human colon carcinoma cells. *Oncol Rep*. 2013;29:1623–8.
- Liu L, Liu T, Tao W, Liao N, Yan Q, Li L, et al. Flavonoids from *Scutellaria Barbata* D. Don exert antitumor activity in colorectal cancer through inhibited autophagy and promoted apoptosis via ATF4/sestrin2 pathway. *Phytomedicine*. 2022;99:154007.
- Xinkui L, Jiarui W, Dan Z, Kaihuan W, Xiaoqiao D, Ziqi M, et al. Network Pharmacology-based Approach to investigate the mechanisms of *Hedyotis Diffusa* Willd. in the treatment of gastric Cancer. *Evid Based Complement Alternat Med*. 2018;2018:1–17.
- Li YL, Zhang J, Min D, Hongyan Z, Lin N, Li QS. Anticancer effects of 1,3-Dihydroxy-2-Methylanthraquinone and the Ethyl acetate fraction of *Hedyotis Diffusa* Willd against HepG2 Carcinoma cells mediated by apoptosis. *PLoS ONE*. 2016;11:e0151502.
- Xu X, Chen F, Zhang L, Liu L, Zhang C, Zhang Z, et al. Exploring the mechanisms of anti-ovarian cancer of *Hedyotis Diffusa* Willd and *Scutellaria Barbata* D. Don through focal adhesion pathway. *J Ethnopharmacol*. 2021;279:114343.
- Son YO, Kook SH, Lee JC. Glycoproteins and Polysaccharides are the Main Class of Active Constituents Required for Lymphocyte Stimulation and Antigen-Specific Immune Response Induction by Traditional Medicinal Herbal Plants. *J Med Food*. 2017;20(10):1011–1021.
- Tecza K, Pamula-Pilat J, Kolosza Z, Radlak N, Grzybowska E. Genetic polymorphisms and gene-dosage effect in ovarian cancer risk and response to paclitaxel/cisplatin chemotherapy. *J Experimental Clin Cancer Res*. 2015;16:34(1)
- Qi L, Luo Q, Zhang Y, Jia F, Wang F. Advances in toxicological research of the anticancer drug cisplatin. *Chem Res Toxicol*. 2019;32.
- Esposito M, Ganesan S, Kang Y. Emerging strategies for treating metastasis. *Nat Cancer*. 2021;2:258–70.
- Yang J, Antin P, Bex G, Blanpain C, Brabletz T, Bronner M, et al. Guidelines and definitions for research on epithelial–mesenchymal transition. *Nat Rev Mol Cell Biol*. 2020;21:341–52.
- Yan X, Zhang Y, Zhang J, Zhang L, Liu Y, Wu Y, et al. p62/SQSTM1 as an onco-target mediates cisplatin resistance through activating RIP1-NF- κ B pathway in human ovarian cancer cells. *Cancer Sci*. 2017;108:1405–13.

30. Yan Y, Zhong R, Yu H, Zhang C, Liu N, Zhang Y et al. p62 aggregates mediated caspase 8 activation is responsible for progression of ovarian cancer. *J Cell Mol Med*. 2019;23(6):4030-4042.
31. Lu J, Ding Y, Zhang W, Qi Y, Zhou J, Xu N, et al. SQSTM1/p62 knockout by using the CRISPR/Cas9 system inhibits migration and invasion of hepatocellular carcinoma; 2023.
32. Chen J, Gao Z, Li X, Shi Y, Tang Z, Liu W et al. SQSTM1/p62 in intrahepatic cholangiocarcinoma promotes tumor progression via epithelial-mesenchymal transition and mitochondrial function maintenance. *Cancer Med*. 2023;12(1):459-471.
33. Xi XX, Wang J, Qin Y, You Y, Huang W, Zhan J. The biphasic effect of flavonoids on oxidative stress and cell proliferation in breast cancer cells. *Antioxidants*. 2022;11.
34. Zhang L, Cheng T, Yang H, Chen J, Wen X, Jiang Z, et al. Interferon regulatory factor-1 regulates cisplatin-induced apoptosis and autophagy in A549 lung cancer cells. *Med Oncol*. 2022;39:1-12.
35. Kepp O, Bezu L, Yamazaki T, Virgilio FD, Galluzzi L. ATP and cancer immunosurveillance. *EMBO J*. 2021;1;40(13):e108130.
36. Ke R, Xu Q, Li C, Luo L, Huang D. Mechanisms of AMPK in the maintenance of ATP balance during energy metabolism. *Cell Biol Int*. 2018;42:384-92.
37. Cheung EC, Vousden KH. The role of ROS in tumour development and progression. *Nat Rev Cancer*. 2022;22.
38. Chiang SK, Chen SE, Chang LC. A dual role of Heme Oxygenase-1 in cancer cells. *Int J Mol Sci*. 2018;21;20(1):39.
39. Dixon S, Lemberg K, Lamprecht M, Skouta R, Zaitsev E, Gleason C et al. Ferroptosis: an iron-dependent form of nonapoptotic cell death. *Cell*. 2012;149.
40. Park E, Chung SW. ROS-mediated autophagy increases intracellular iron levels and ferroptosis by ferritin and transferrin receptor regulation. *Cell Death Dis*. 2019;10.
41. Sun K, Li C, Liao S, Yao X, Ouyang Y, Liu Y, et al. Ferritinophagy, a form of autophagic ferroptosis: new insights into cancer treatment. *Front Pharmacol*. 2022;13:1043344.
42. Yanhua, Mou, Jun W, Jinchun W et al. Ferroptosis, a new form of cell death: opportunities and challenges in cancer. *J Hematol Oncol*. 2019;29;12(1):34.
43. Mancias JD, Wang X, Gygi SP, Harper JW, Kimmelman AC. Quantitative proteomics identifies NCOA4 as the cargo receptor mediating ferritinophagy. *Nature*. 2014;509:105-9.
44. Jin Y, Qiu J, Lu X, Li G. C-MYC inhibited ferroptosis and promoted immune evasion in ovarian cancer cells through NCOA4 mediated ferritin autophagy. *Cells*. 2022;11:4127.
45. Loboda A, Damulewicz M, Pyza E, Jozkowicz A, Dulak J. Role of Nrf2/HO-1 system in development, oxidative stress response and diseases: an evolutionarily conserved mechanism. *Cell Mol Life Sci*. 2016;73:3221-47.
46. Jiang T, Harder B, De La Rojo M, Wong PK, Chapman E, Zhang DD. p62 links autophagy and Nrf2 signaling. *Free Radic Biol Med*. 2015;88:199-204.
47. Yang S, Li F, Lu S, Ren L, Bian S, Liu M, et al. Ginseng root extract attenuates inflammation by inhibiting the MAPK/NF- κ B signaling pathway and activating autophagy and p62-Nrf2-Keap1 signaling in vitro and in vivo. *J Ethnopharmacol*. 2022;283:114739.
48. Hong Y, Liu J, Kong W, Li H, Cui Y, Liu Y, et al. WASH regulates the oxidative stress Nrf2/ARE pathway to inhibit proliferation and promote apoptosis of HeLa cells under the action of Jolkinolide B. *PeerJ*. 2022;10:e13499.
49. Sun X, Li J, Li Y, Wang S, Li Q. Apatinib, a novel tyrosine kinase inhibitor, promotes ROS-Dependent apoptosis and autophagy via the Nrf2/HO-1 pathway in Ovarian Cancer cells. *Oxid Med Cell Longev*. 2020;13:2020:3145182.
50. Yu H, Chen B, Ren Q. Baicalin relieves hypoxia-aroused H9c2 cell apoptosis by activating Nrf2/HO-1-mediated HIF1 α /BNIP3 pathway. *Artif Cells*. 2019;47:3657-63.
51. Wei R, Zhao Y, Wang J, Yang X, Li S, Wang Y, et al. Tagitinin C induces ferroptosis through PERK-Nrf2-HO-1 signaling pathway in colorectal cancer cells. *Int J Biol Sci*. 2021;17:2703-17.

Publisher's note

Springer Nature remains neutral with regard to jurisdictional claims in published maps and institutional affiliations.